Mofidi A, Cheng L, Chaallal O, Shao Y.

Shear strengthening of RC beams with NSM FRP—Influencing parameters and a theoretical model.

American Concrete Institute Special Publication 2018, 327, 31.1-31.16.

Shear Strengthening of RC Beams with NSM FRP — Influencing Parameters and A Theoretical Model

Amir Mofidi, Lijuan Cheng, Omar Chaallal, Yixin Shao

Synopsis: This paper evaluates the influence of the key parameters on the shear behavior of reinforced concrete (RC) beams retrofitted in shear using near-surface mounted (NSM) fiber-reinforced polymers (FRP) laminates and rods. The commonly observed debonding failure is considered in the study. The principal bond related parameters are examined, including the FRP effective bond length, the NSM FRP to concrete bond relation and the pull-off force of NSM FRP bonded from concrete surface. It is found that unlike the beams strengthened with externally bonded (EB) FRP, the effect of the existing transverse steel shear reinforcement on the shear contribution of FRP is not significant and should not be considered by the design models. The existing experimental results in the open literature also show that the internal steel shear reinforcement and the strengthening NSM FRP do not diminish each other's contributions to the shear resistance of the RC beam. To precisely predict the shear contribution of NSM FRP of the strengthened RC beams corresponding to the debonding failure, a new prediction method is proposed in this study to consider the most influencing factors on the shear contribution of NSM FRP (V_f). The accuracy of the proposed equations is verified by comparing the predictions with the shear strength of a series of experimentally tested RC beams from the literature. Moreover, a comparison with other existing models shows that the proposed model achieves a better correlation with the experimental data than the other existing equations.

Click here to download accompanying video

Keywords: Fiber-reinforced polymer (FRP); near-surface mounted (NSM); shear; concrete; steel reinforcement

Amir Mofidi is a Postdoctoral Fellow and a Lecturer in the Department of Civil Engineering and Applied Mechanics at McGill University. He is a voting member of ACI 440F Subcommittee. His research interests include use of fiber-reinforced polymer composites for strengthening and retrofitting concrete structures.

Lijuan "Dawn" Cheng is an Associate Professor in the Department of Civil and Environmental Engineering at the University of California, Davis. She is a member of ACI Committee 440, Fiber Reinforced Polymer Reinforcement, ASCE, TRB, and IIFC. Her research interest includes innovative infrastructures and rehabilitation using advanced composite materials, large-scale testing and numerical simulations, design, analysis and durability of fiber reinforced polymer composites, etc.

Omar Chaallal, FACI, is a Professor of Construction Engineering at University of Quebec, Ecole de Technologie Supérieure, Montreal, Canada. He is a member of ACI Committee 440, Fiber Reinforced Polymer Reinforcement. He chairs the CSA-S806 TSC on shear strengthening. His research interests include experimental and analytical research on the use of fiber reinforced polymer composites for strengthening and repair of concrete structures.

Yixin Shao, FACI, is a Professor in the Department of Civil Engineering and Applied Mechanics at McGill University. He received his PhD from Northwestern University, Evanston, IL. His research interests include use of advanced composites in construction, carbonation curing of concrete, use of wastes, environmentally friendly building materials, and durability.

INTRODUCTION

Rehabilitation of existing reinforced concrete structures using advanced composites has gained much attention among researchers and engineers in recent decades. In addition to other strengthening methods, rehabilitation of reinforced concrete beams using Near-Surface Mounted (NSM) Fiber-Reinforced Polymers (FRP) has received noticeable attention. Use of NSM steel rods grouted to a bridge slab to strengthen the slab in flexure was first proposed by Asplund [1]. Later, Nanni *et al.* [2] used NSM FRP rods to strengthen a highway bridge in flexure. The use of NSM FRP reinforcement for strengthening RC beams and slabs in flexure is well established. In recent years, an outstanding research effort has been undertaken with a view to understand the behavior of NSM FRP used for shear strengthening of concrete structures. However, because of its complexity, the shear strengthening of RC members with NSM FRP requires further investigation. Between 2001 and 2015, many research studies on the shear strengthening of RC beams with NSM FRP composites were carried out [3-15]. The results of these studies led to different design equations and analytical models to predict the shear contribution of NSM FRP. However, several major influencing parameters related to the shear strengthening using NSM FRP have not been captured by those existing theoretical predictive tools.

The first category of the major influencing parameters is related to the formulation of the bond behavior of NSM FRP to concrete. In general, the bond behavior of FRP should be calculated in association with a logical and accurate bond model between NSM FRP and concrete surface. So far, different bond models have been proposed by researchers, but the bond models have not been incorporated into practical equations for the current design models.

The second category of key influencing parameters is related to the anchorage length of the NSM FRP. In general, the effective anchorage length of NSM FRP is significantly longer than that of Externally Bonded (EB) FRP. Therefore, the effective anchorage length of the NSM FRP might not be provided for all of the strengthening NSM FRP installed in RC beams' web. This effect has not been recognized and addressed so far in the existing studies related to shear strengthening with NSM FRP.

The third category is related to the effect of existing shear transverse steel reinforcement (stirrups) on NSM FRP debonding. Recent findings have highlighted the effect of shear steel reinforcement on FRP contribution in shear strengthening with EB FRP [e.g., 16-18]. Although this effect was claimed insignificant in previous studies on RC beams shear strengthened with NSM FRP [3, 15], these parameters are insufficiently documented. Whether or not a quantifiable relationship exists is doubtful between the transverse steel reinforcement and NSM FRP shear contribution.

In this regard, after a review of the most influential parameters introduced earlier on the debonding failure mode of RC beams strengthened with NSM FRP, a new prediction tool that considers the most effective factors on the contribution of FRP to the shear resistance is proposed in this paper.

RESEARCH SIGNIFICANCE

Several important questions still remain unanswered regarding the bond behavior and debonding failure mode of RC beams strengthened in shear using NSM FRP. Under the motivation of these research needs, this study aims at evaluating the effect of influencing parameters that have not been sufficiently documented in the current literature and design models. The possible effect due to internal transverse steel reinforcement on NSM FRP shear contribution is also investigated. Based on the results of this study, a theoretical model with practical equations is proposed for predicting the shear resistance of NSM FRP-strengthened RC beams. The accuracy of the proposed equations is verified using a large set of experimental data in the literature. The proposed model is also compared with other design models in the existing literature to demonstrate its unique advantages.

CONTRIBUTION OF NSM FRP TO SHEAR RESISTANCE

The nominal shear resistance at the ultimate limit state, V_n, of RC beams retrofitted in shear with NSM FRP is generally calculated simply by adding the contribution of FRP to the shear resistance, V_f, to that of concrete, V_c, and of steel, V_s, as follows:

$$V_n = V_c + V_s + V_f \tag{1}$$

The contributions of concrete and transverse steel are calculated using the design guidelines for non-strengthened RC structures, assuming that the FRP strengthening does not influence the shear contribution of the concrete or of the transverse steel reinforcement. To calculate the FRP contribution to shear resistance, most existing models [e.g., 5, 12] use the same truss analogy as that used to calculate the contribution of steel stirrups. Thus, the shear contribution of FRP is obtained by multiplying the ultimate vertical stress in the NSM FRP by the area of the NSM FRP laminates or rods that cross a potential shear crack. All the NSM FRP that are intersected by the selected shear crack are assumed to contribute the same to the FRP effective strain. However, a question remains to be answered, whether the anchorage length of all NSM FRP intersected by the crack is sufficient to effectively contribute to the shear resistance at the ultimate? The important concept of NSM FRP effective bond length, defined as the length beyond which the bond capacity remains constant, plays a key role to answer this particular question. In the next section, the key parameters influencing the bonding capacity of the NSM FRP to concrete including the effective bond length of NSM FRP are discussed. The findings will help to better understand the shear behavior of RC beams strengthened with NSM FRP including the abovementioned key question, and to develop a rational, accurate and practical model to predict the shear behavior of RC beams strengthened with NSM FRP laminated and rods.

IMPORTANT FACTORS INFLUENCING NSM FRP DEBONDING IN SHEAR

The debonding of FRP is reported to be the most likely governing failure mode for RC beams shear-strengthened with NSM FRP. However, most of the existing analytical models for shear strengthening of RC beams with NSM FRP do not use any bond models to predict the debonding of NSM from concrete. The existing analytical models still use fixed values or empirical equations to calculate FRP strain. In order to better investigate the parameters related to bonding of NSM FRP to concrete as well as other influencing parameters observed during the experiments, a database of 69 RC beams shear strengthened with NSM FRP laminates and rods is selected (see Mofidi *et al.* [15] for the database). The database includes most of the relevant data in the existing literature of the tested beams strengthened with NSM FRP varying in geometric properties of the test specimens and FRP composites, the elastic and mechanical properties of the materials used, the load at failure (V_{total}), and the contribution of the FRP to shear resistance (V_f).

Figure 1 shows the number of beam specimens using NSM FRP laminates and rods among the 69 RC beams in the database with respect to each observed failure mode. The failure modes are abbreviated as follows: transverse concrete cover splitting (CSF), longitudinal cover detachment or splitting (LCS), FRP debonding (DBN), FRP fracture (FFF), diagonal tension failure (DTF), concrete crushing (CCF), and flexural failure (FLX). It can be seen that, among the specimens using NSM FRP laminates and rods, the debonding is the most probable failure mode, i.e., 43% of the beam specimens failed due to this type of mode. Thus, the bond characteristics of NSM FRP-concrete interface is among the most important parameters that should be investigated but have not yet been captured by most existing design models. It is believed that an inclusive, rational, and practical model is attainable given the body of research in the field. Before developing such a conceptual model, a brief review of the influencing factors is provided in this section.

Bond model

Several researchers have proposed various bond models based on experimental studies on NSM FRP to concrete joint tests. De Lorenzis [19] conducted valuable tests considering different FRP material, shape and groove configuration on NSM FRP rods-to-concrete joints. She proposed different local bond stress-slip relationships for NSM FRP-to-concrete joints for different test variables. It was concluded that a general bond-slip model that considers geometry and material property functions should be developed [20]. Seracino *et al.* [21] proposed a generic analytical model to predict the debonding resistance of adhesively bonded plate-to-concrete joint using an idealized linear-softening local interface bond-slip relationship, which is applicable to NSM FRP-concrete joints. It should be noted that most of the existing design equations to predict the shear contribution of NSM FRP for shear strengthened RC beams do not incorporate a logical bond model.

Effective strain

Assuming that the NSM FRP reinforcement carries only normal stresses in the principal FRP material direction, NSM FRP may be treated by a similar analogy to the transverse steel stirrups. In this case, all FRP laminates or rods intersected by the selected shear crack are assumed to contribute the same to the FRP effective strain (if certain anchorage length is provided for all NSM FRP intersected by the crack). The effective strain, ε_{fe}, in the principal material direction is in general less than the tensile strain at failure, ε_{fu}.

In recent years, researchers have proposed various equations to calculate this effective strain, ε_{fe} [e.g., 5, 10 and 11]. However, none of the existing equations incorporates a reliable bond model. In the new model proposed in this study, taking advantage of a state-of-the-art bond model by Seracino *et al.* [21], the effective strain in the FRP is calculated using the equilibrium conditions in the NSM FRP rods or laminates. Prior to debonding, the force in the FRP is equal to the maximum bonding force between the FRP and the concrete surface (taken equal to the pull-off force, P_{fb}, calculated using the model by Seracino *et al.* [21]). The force that can be developed in the NSM FRP on one side of the beam can be calculated using the bond model. The effective strain corresponding to FRP debonding is calculated afterwards as follows:

$$P_{fb} = A_f.E_f.\varepsilon_{fe} \tag{2}$$

It follows that:

$$\varepsilon_{fe} = \frac{P_{fb}}{A_f.E_f} \tag{3}$$

FRP effective anchorage length

Empirically, for NSM FRP with an FRP anchorage length greater than the effective bond length, the ultimate tensile force is limited to the force corresponding to the effective anchorage length. This implies that the bond capacity does not increase constantly and boundlessly with the bond length. This explains the rationale behind the important concept of effective bond length, defined as the length beyond which the bond capacity remains constant.

For NSM FRP laminates, Seracino *et al.* [21] proposed equations based on a bi-linear fracture mechanics model to calculate the effective bond length as follows:

$$L_{ef} = \frac{\pi}{2\lambda} \tag{4}$$

$$\lambda^2 = \frac{\tau_{\max} L_{per}}{\delta_{\max} E_f A_f} \tag{5}$$

where $\tau_{\max}$ and $\delta_{\max}$ are, respectively, the maximum shear stress and the maximum slip, assuming a bilinear bond-slip relationship at the concrete-epoxy interface. The maximum shear stress and maximum slip are calculated on the basis of an empirical equation extracted from a statistical analysis [22]. That is,

$$\tau_{\max} = (0.802 + 0.078\varphi_f)\, f_c'^{\,0.6} \tag{6}$$

$$\delta_{\max} = \frac{0.976\varphi_f^{\,0.526}}{0.802 + 0.078\varphi_f} \tag{7}$$

where units of Newton and millimeter are used (1 Newton is equal to 0.225 Pound-force and 1 mm is equal to 0.039 inches). φ_f is the debonding-failure plane aspect ratio that is equal to $(d_f)/(b_f)$. d_f is the length of the failure plane perpendicular to the concrete surface, which for NSM plates is taken to be the depth of the groove plus 1 mm (0.039 inches). b_f is the length of the failure plane parallel to the concrete surface (at the FRP-concrete interface), which for NSM laminates and rods is taken to be the width of the groove plus 2 mm (0.078 inches). The width and depth of the groove in this study are taken as 1.5 times the rod diameter based on pull-off tests of Wiwatrojanagul *et al.* [13]. The other important parameter in Eq. (5) is L_{per}, which is the debonding failure plane in the cross-section and is set equal to $(2d_f + b_f)$ under the assumption that the effective bond length (L_{ef}) of the FRP laminates or rods is fully available.

The maximum available FRP anchorage length, L_{max}, is a parameter dependent on the RC beams size. In fact, L_{max} is limited by the concrete beam's cross-sectional size and is equal to $d_v/2\sin\alpha$, where d_v is the effective shear depth and can be taken as the greater of 0.72h and 0.9d as per CSA/S806 [23]. This is due to the fact that for NSM FRP laminates and rods the bond lengths should be sought on both sides of the major crack line to ensure a successful bond. Based on the data gathered, of all strengthened RC beams in the database, only in 17% of the beams the available anchorage length of at least one NSM FRP is attainable ($L_{max} \geq L_{ef}$) in both sides of the principle shear crack. This means that in the majority of the specimens (83%) none of the NSM FRP laminate or rods reached the maximum bonding capacity prior to debonding since $L_{max} < L_{ef}$. In the most recent design models for shear strengthening of RC beams with externally-bonded (EB) FRP fabrics, the fibers that do not have an anchorage length longer than the effective length are disregarded in calculations of shear contribution of EB FRP [e.g., 24-25]. However, in beams strengthened with NSM FRP, in the majority of specimens none of the NSM FRP reached the effective anchorage length of the laminates or rods. This is due to the fact that the effective length of NSM FRP laminates and rods are considerably longer compared to that of the EB FRP fabrics and strips. The average calculated effective length of the NSM FRP gathered in our database is 263 mm, whereas the average effective length of the EB FRP fabrics and strips gathered by Mofidi and Chaallal [25] is 90 mm. Therefore, it is imperative to find a way to calculate the contribution of NSM FRP to the shear resistance when the anchorage length of the NSM FRP intercepted by the major shear crack is smaller than the effective bond length of the NSM FRP. The newly proposed model presented in the following section considers a solution to address this issue in beams with $L_{max} < L_{ef}$.

Transverse steel

Experimental tests have revealed that EB FRP composites are less effective when beams are heavily reinforced with internal shear-steel reinforcement [26-27]. It has been clearly established that the effectiveness of the strengthening FRP changes with the amount of internal shear-steel reinforcement. In this regard, design equations to calculate the shear contribution of EB FRP have been proposed that incorporate the diminishing effect of the existing shear-steel reinforcement [23-24]. A question to be answered is whether or not a similar diminishing effect by the shear-steel reinforcement applies to the NSM FRP? In order to answer this question, the average variations in the FRP shear contribution for NSM-strengthened RC beams in the database are plotted against the different ranges of internal steel stirrup ratios in Figure 2. The ratio is defined as $\rho_{sv} = A_{sv}/(b_w \times s)$, where A_{sv} and s are the total area of the cross-section and the spacing of the transverse steel reinforcement. The specimens are categorized in four groups: RC beams with no steel stirrups ($\rho_{sv} = 0$); RC beams with light transverse steel reinforcement ($\rho_{sv} < 0.125$); RC beams with moderate transverse steel reinforcement ($0.125 \leq \rho_{sv} \leq 0.175$); and RC beams with heavy transverse steel reinforcement ($\rho_{sv} > 0.175$).

It can be seen that the average NSM FRP shear contribution increases slowly when the steel shear reinforcement ratio increases up to 0.175. Unlike the EB FRP method, the presence of the internal steel stirrups does not seem to adversely affect the contribution of FRP to the shear resistance in the NSM method. As opposed to what is observed in the EB FRP method, the highly stressed areas around NSM FRP do not significantly overlap and interact with the highly stressed areas around the existing steel stirrups. This is mainly due to the fact that the location of the NSM FRP reinforcement is generally taken with distance away from the location of steel stirrups to avoid possible damage to the existing steel stirrups during groove cutting for NSM FRP. Therefore, the bond quality between the NSM FRP and the concrete is not compromised by the presence of the steel stirrup. Moreover, the presence of steel stirrups in those beams eases the stresses in the NSM FRP laminates or rods and the adjacent concrete zones as compared to similar beams without internal stirrups. These findings are particularly in correlation with the experimental results obtained by De Lorenzis and Nanni [3] and Mofidi *et al.* [15], where the presence of the transverse steel shear reinforcement is one of the test variables.

To verify lack of considerable interaction between the internal transverse steel reinforcement and the NSM FRP used for strengthening of RC beams in shear, experimental results of 6 beams reported in Mofidi *et al.* [15] are analyzed in more depth. In this study, the control specimens not strengthened with carbon FRP rods are labeled as CON. The specimens labeled as NR are RC T-beams with no internal transverse steel stirrups. The specimens labeled as MR (moderately reinforced with internal transverse steel reinforcement) and HR (heavily reinforced with internal transverse steel reinforcement) have steel stirrups spaced at $s = 3d/4$ for MR and $s = d/2$ for HR, where $d = 350$ mm is the effective depth of the beam cross-section. The specimens strengthened with NSM are labeled as NSM. The spacing between the NSM FRP rods is 130 mm for all strengthened specimens. The experimental contributions of transverse steel and NSM FRP reinforcement are calculated as the sum of the contributions corresponding to the stirrups and NSM FRP rods crossing the plane of rupture, respectively.

In order to further investigate this effect, the FRP shear contribution of each strengthened specimen with respect to the applied shear is displayed in Figure 3. It can be seen from Figure 3 that among the strengthened beams that failed in shear (NR-NSM and MR-NSM), the shear contribution of FRP is slightly greater in the specimen with transverse steel reinforcement compared to that of the specimen without transverse steel reinforcement (44 kN versus 39 kN, correspondingly). This indicates that V_f does not decrease with the addition of the steel stirrups. Therefore, it can be concluded that the presence of the transverse steel reinforcement does not have a diminishing effect on the NSM FRP.

Figure 4 shows the transverse steel contribution to the shear capacity (V_s) with respect to the applied shear force on the beams under 3-point static loading (slender beams). When comparing V_s of a strengthened beam with that of the corresponding control beam, the presence of the gray zones (MR and HR zones) can be attributed to the addition of the NSM FRP to the strengthened specimens (Figure 4). As the FRP is added to a strengthened specimen, the strain in the transverse steel reinforcement (and hence the shear contribution of steel) is eased downed compared to that in the corresponding control specimens. The difference in the shear contribution of the transverse steel reinforcement between the strengthened specimen and the control specimen of each series (MR and HR series) while the applied shear is between 100 kN to 250 kN (1 kN is equal to 0.225 kip) creates the gray zones corresponding to each beam series (Figure 4). It is clear that the difference in the shear contribution of similar strengthened and control specimens can be attributed to the strengthening NSM FRP material. The similarity of the two zones implies that the differences in the ratio of transverse steel reinforcement do not affect the shear contribution of FRP significantly (V_f).

On the other hand, it is instructive to investigate whether the presence of the NSM FRP diminishes the effectiveness of the existing steel shear reinforcement. Figure 4 reveals that V_s is greater in the control specimens when the applied shear is between 100 kN to 250 kN. However, prior to failure, V_s is greater in the strengthened specimens compared to their corresponding control specimens. It can be concluded that the addition of the NSM FRP does not attenuate the shear contribution of the transverse steel reinforcement.

Based on the results of this section, a new model is proposed to calculate the shear contribution of FRP due to debonding of NSM FRP that is independent of the existing steel shear reinforcement properties of the RC beam. This is due to the fact that such interaction between the existing steel shear reinforcement and strengthening FRP, which was previously observed and rationalized by researchers for RC beams strengthened with EB FRP, do not exist for specimens strengthened in shear with NSM FRP.

PROPOSED THEORETICAL MODEL

In this section, a new theoretical model with practical equations is developed for predicting the shear contribution of NSM FRP of RC beams strengthened in shear using NSM FRP laminates and rods. The proposed equations account for various key parameters discussed previously. The new model proposed in this article is a modification to the model proposed by Mofidi *et al.* [15] in terms of ease of use, precision of the predicted results, and calculation method of the sum of NSM FRP that effectively contribute to the shear resistance at the ultimate debonding failure (n_f).

The shear force resisted by the NSM FRP can be calculated as the sum of the forces resisted by the intersected NSM FRP laminates and rods by the major shear crack that effectively contribute to the shear resistance at the ultimate failure, i.e.,

$$V_f = 2\sum A_f f_f = 2n_f A_f E_f \varepsilon_{ef} \tag{8}$$

where A_f is the cross-sectional area of the laminates or rods; f_f is the ultimate vertical tensile stress in the NSM FRP laminates or rods at the crack; and E_f is the modulus of elastic of the NSM FRP.

As mentioned earlier the effective strain of NSM FRP laminates and rods with anchorage length greater than the effective length can be calculated using the pull-off force (P_{fb}) of the NSM FRP proposed by Seracino *et al.* [21] bond model as follows:

$$P_{fb} = 0.85\varphi_f^{\,0.25} \cdot f_c'^{\,0.33} \sqrt{L_{per} E_f A_f} \tag{9}$$

Hence, substituting the above equation in Eq. (3), the effective strain in the effectively bonded NSM FRP laminates and rods (minimum anchorage length is equal to L_{ef}) can be calculated using the following equation:

$$\varepsilon_{ef} = \frac{0.4\varphi_f^{\,0.25} \cdot f_c'^{\,0.33} \sqrt{L_{per}}}{\sqrt{E_f A_f}} \tag{10}$$

As suggested by Seracino *et al.* [21], the pull-off force of the NSM FRP is a linear function of the smaller bond length of NSM FRP laminates or rods, where the effective bond length represents the upper bound of FRP bond length. The calculated pull-off force by Eq. (9) is valid under the assumption that the effective bond length (L_{ef}) of the FRP laminates or rods is fully available. As discussed earlier, for RC beams strengthened in shear with NSM FRP in the database, the effective length of the FRP was only physically available for 17% of the specimens (depending on the geometry of the concrete cross-section and the inclination of the NSM FRP). Considering the physical availability of the effective anchorage length, it is important to know the number of the NSM FRP laminates and rods that effectively contribute to the shear resistance at the ultimate failure for the following two cases:

(1) If $\dfrac{d_v}{2\sin\alpha} \geq L_{ef}$:

In the case where $L_{max} \geq L_{ef}$, the maximum FRP stress occurs in those NSM FRP that have a bond length at least equal to the effective bond length. After a major shear crack propagates through a beam's cross section, only the NSM FRP that have an anchorage length greater than the FRP effective length remain adequately anchored. Therefore, a certain number of the NSM FRP laminates or rods (n_f) reach their maximum bonding capacity. These NSM FRP laminates or rods are the only strengthening NSM FRP that contribute to the shear resistance until the ultimate failure due to debonding. The other NSM FRP laminate or rods that are not anchored at least as long as the effective bond length will debond prior to the ultimate failure. The later NSM FRP should not be considered in the calculation of the shear contribution of FRP, regardless of the fact that they intersect the major shear crack. On the other hand, for NSM FRP with anchorage lengths greater than L_{ef}, n_f is calculated from the following equation which calculates the total number of the NSM FRP intercepted by the major shear crack subtracted by the number of NSM FRP with anchorage length smaller than L_{ef} as follows:

$$n_f = 1 + \frac{d_v - (L_{ef}/\sin\alpha)}{s_f} \tag{11}$$

where $(d_v - L_{ef}/\sin\alpha)/s_f$ is the number of spacings between the NSM FRP that effectively contribute to the shear resistance at the ultimate.

(2) If $\dfrac{d_v}{2\sin\alpha} < L_{ef}$

In the case where $L_{max} < L_{ef}$, the anchorage length of none of the NSM FRP are as long as the effective bonding length. However, FRP stresses still develop in the NSM FRP intersected by the major shear crack. The amount of the NSM FRP stresses are in direct relation with the smaller anchorage length of the NSM FRP with respect to the shear crack intersection point. On each side of the major shear crack, one NSM FRP contributes to the shear resistance with the longest anchorage length compared to the other NSM FRP until the ultimate debonding failure occurs. At the ultimate failure only the NSM FRP with the longest anchorage length at each side of the crack will effectively contribute to the shear resistance. The developed FRP stress at ultimate in the two NSM FRP (one NSM FRP each side of the major shear crack) is a ratio of the maximum FRP stresses calculated by the Seracino *et al.* [21] model. The later ratio is equal to total length of NSM FRP with longer anchorage lengths on each side of the major shear crack ($d_v/\sin\alpha - k_p s_f$) divided by effective bond length of the FRP. Therefore, the equivalate number of the NSM FRP that can reach maximum FRP strain (Eq. 3) can be calculated as follows:

$$n_f = \frac{d_v/\sin\alpha - k_p s_f}{L_{ef}} \tag{12}$$

where k_p is an empirical coefficient regarding the spacing between the NSM FRP with the longest anchorage length on each side of the principle shear crack based on the available test results in our database of RC beams strengthened in shear with NSM FRP which is equal to 0.9 and 0.5 for NSM FRP laminates and rods, respectively.

VALIDATION OF THE PROPOSED MODEL

In this section, the predicted V_f by the proposed model for the specimens in the database are compared with the experimental results. Certain specimens are not considered in the comparison for the following reasons: 1) the NSM FRP did not contribute considerably to shear resistance; 2) the specimens failed due to unrelated failure modes to the shear failure; and 3) the specimens benefited from a special anchorage of NSM FRP.

The accuracy of the proposed model to calculate V_f is demonstrated by the comparison with that of the existing design models by De Lorenzis and Nanni [3], Dias and Barros [10], and Anwarul Islam [11] (Table 1). It should be noted that the model by De Lorenzis and Nanni [3] can only predict results of RC beams strengthened with NSM FRP rods. The model proposed by Dias and Barros [10] can only predict results for RC beams strengthened with NSM FRP laminates. For more details on the comparison of calculated results by De Lorenzis and Nanni [3], Dias and Barros [10], and Anwarul Islam [11] with experimental results see Mofidi *et al.* [15]. Figures 5 to 7 compare the predicted values of shear contribution of NSM FRP using the proposed model ($V_{f\,cal}$) with the experimental results ($V_{f\,exp}$) of all strengthened specimens for NSM laminates and NSM rods, respectively. It can be seen that the proposed model's accuracy is superior to the existing design models (overall R^2 = 0.64). When the FRP laminate and rod cases are considered separately, the proposed model predicts V_f for strengthened beams with R^2 = 0.67 and R^2 = 0.65 for beams with laminates and rods, respectively.

SUMMARY AND CONCLUDING REMARKS

The major parameters affecting the shear contribution of NSM FRP and the role of these parameters in the shear behavior of RC beams strengthened with NSM are evaluated in this paper. The assessment using the existing experimental results in the database shows that parameters such as effective bond length and effective strain of NSM FRP play a key role to predict the behavior of shear-strengthened RC beams with NSM FRP. A logical bond model, which is currently lacked in most existing design models, is found to be a necessity to predict the shear contribution of NSM FRP. On the basis of this effort, a new design model is proposed for predicting the shear contribution of NSM FRP, using a state-of-the-art bond model proposed by Seracino *et al* [21]. The effectiveness of the proposed method is demonstrated using the experimental results available in the literature. The proposed model showed a superior correlation with experimental results in comparison with other existing models. From this study, the following conclusions can be drawn:

- The influence of conventional transverse-steel shear reinforcement on the contribution of NSM FRP to shear resistance is proved to be insignificant. The experimental results by the authors and analysis of the results in the database shows that, unlike what it was observed for RC beam strengthened with EB FRP, the interaction between the existing shear steel reinforcement and NSM FRP hardly exists;
- A new approach in predicting the NSM FRP shear contribution is proposed, where only the NSM FRP laminates and rods that effectively contribute to the shear resistance at the ultimate are considered; and
- In the proposed model, only NSM FRP laminates or rods that are anchored with minimum effective bond length of NSM FRP are considered. If based on the geometry of the RC beam none of NSM FRP are anchored with minimum L_{ef}, only one NSM FRP on each side of the principle crack with the longest anchorage length is considered in predicting the V_f.

ACKNOWLEDGMENTS

The authors acknowledge the support provided by Mitacs, Sika AG and Sika Canada Inc. through a Mitacs postdoctoral fellowship to Dr. Mofidi, by the University of California, Davis, for partial financial support of the research. The first author particularly thanks Mr. Thierry Berset and Ms. Annika Baier at Sika AG, and Mr. Philippe Guevremont, Mr. Jonathan Clavet, and Mr. Bob Barham at Sika Canada Inc. for their valuable contributions to this research.

LIST OF NOTATIONS

The following symbols are used in this paper:

A_f	=	cross-sectional area of NSM FRP;
A_{sv}	=	cross-sectional area of steel stirrups;
b_f	=	the length of the failure plane parallel to the concrete surface (at the FRP/concrete interface);
d	=	effective depth of the RC beam's cross-section;
d_f	=	the length of the failure plane perpendicular to the concrete surface;
d_v	=	the greater of 0.72h and 0.9d;
E_f	=	modulus of elasticity of NSM FRP;
f_f	=	ultimate vertical tensile stress in NSM FRP;
h	=	RC beam's cross-sectional height;
k_p	=	empirical coefficient regarding the spacing between effective NSM FRP when $L_{max} < L_{ef}$;
L_{ef}	=	effective length of NSM FRP;
L_{max}	=	maximum available anchorage length;
L_{per}	=	the debonding failure plane in the cross-section;
n_f	=	number of NSM FRP effectively contributing to the shear resistance at the ultimate failure;
P_{fb}	=	pull-off force of NSM FRP bonded to concrete;
s	=	the spacing of the transverse steel reinforcement;
V_c	=	the shear contribution of concrete;
V_f	=	the shear contribution of NSM FRP;
$V_{f\,cal}$	=	calculated shear contribution of NSM FRP;
$V_{f\,exp}$	=	experimental shear contribution of NSM FRP;
V_n	=	nominal shear resistance at the ultimate limit state;
V_s	=	the shear contribution of existing steel shear reinforcement;
V_{total}	=	the shear contribution of NSM FRP;
α	=	NSM FRP inclination;
$\delta_{\max}$	=	maximum slip assuming a bilinear bond-slip relationship at concrete/epoxy interface;
ε_{fe}	=	NSM FRP effective strain;
ε_{fu}	=	ultimate strain of FRP
φ_f	=	debonding-failure plane aspect ratio;
ρ_{sv}	=	$A_{sv} /(b_w \times s)$;
$\tau_{\max}$	=	maximum shear stress assuming a bilinear bond-slip relationship at concrete/epoxy interface.

REFERENCES

[1] Asplund, S.O, 1949, "Strengthening bridge slabs with grouted reinforcement", ACI Struct J 20(5), 397–406.

[2] Nanni, A., Alkhrdaji, T., Barker, M., Chen, G., Mayo, R., and Yang, X., 1999, "Overview of testing to failure program of a highway bridge strengthened with FRP composites", Proc of the Fourth Int Symp on Non-Metallic (FRP) Reinforcement for Concrete Structures (FRPRCS-4), SP-188, American Concrete Institute, Farmington Hills. MI, 69–75.

[3] De Lorenzis, L., and Nanni, A., 2001, "Shear strengthening of reinforced concrete beams with NSM fibre-reinforced polymer rods", ACI Struct J 98(1), 60–68.

[4] Rizzo, A., and De Lorenzis, L., 2007, "Behaviour and capacity of RC beams strengthened in shear with NSM FRP reinforcement", Constr Build Mater 23, 1555–1567.

[5] Kotynia, R., 2007, "Shear strengthening of RC beams with NSM CFRP laminates", Proc. of the 8th symposium of fibre-reinforced polymers in reinforced concrete structures, University of Patras, Patras, Greece.

[6] Dias, S.J.E., and Barros, J.A.O. 2008, "Shear strengthening of T-cross section reinforced concrete beams by near-surface mounted technique", J Compos Constr 12(3), 300–311.

[7] Dias, S.J.E., and Barros, J.A.O., 2010, "Performance of reinforced-concrete T-beams strengthened in shear with NSM CFRP laminates", Eng Struct 32, 373–384.

[8] Dias, S.J.E., and Barros, J.A.O., 2011, “Shear strengthening of RC T-section beams with low-strength concrete using NSM CFRP laminates”, Cem Concr Compos 33, 334–345.

[9] Dias, S.J.E., and Barros, J.A.O., 2012, “NSM shear-strengthening technique with CFRP laminates applied in high-strength concrete beams with or without pre-cracking”, Composites: Part B 43, 290–301.

[10] Dias, S.J.E., and Barros, J.A.O., 2013, “Shear strengthening of RC beams with NSM CFRP laminates: Experimental research and analytical formulation”, Compos. Struct. 99, 477-490.

[11] Anwarul Islam, A.K.M., 2009, “Effective methods of using CFRP bars in shear strengthening of concrete girders”, Eng Struct 31, 709–714.

[12] Rahal, K.N., and Rumaih, H.A., 2011, “Tests on reinforced concrete beams strengthened in shear using near surface mounted CFRP and steel bars”, Eng Struct 33, 53–62.

[13] Wiwatrojanagul, P., Ayudhya, B.I.N., and Sahamitmongkol, R., 2012, “NSM FRP shear strengthening of RC beams with internal stirrups”, Thammasat Int J of Scien and Tech 17(1), 16–30.

[14] Raj, S.D., and Surumi, R.S., 2012, “Shear strengthening of reinforced concrete beams using near surface mounted glass fibre reinforced polymer”, Asian J of Civil Eng (Building and housing) 13(5), 679–690.

[15] Mofidi, A., Chaallal, O., Cheng, L., and Shao, Y., 2015, “Investigation of Near-Surface Mounted Method for Shear Rehabilitation of Reinforced Concrete T-Beams using CFRP Rods”, American Society of Civil Engineers (ASCE), Journal of Composites for Construction. 04015048.

[16] Mofidi, A. and Chaallal, O., 2014, “Effect of Steel Stirrups on the Shear Resistance Gain Due to EB FRP Strips and Sheets”, ACI Struct. J. 111(2), 353-362.

[17] Mofidi, A. and Chaallal, O., 2014, “Tests and Design Provisions for Reinforced-Concrete Beams Strengthened in Shear using FRP Sheets and Strips”, International Journal of Concrete Structures and Materials. 8(2), 117-128.

[18] Mofidi, A. and Chaallal, O., 2014, “Reinforced-Concrete Beams Retrofitted in Shear with Externally-Bonded FRP: Development of a Design Model”, Australian Journal of Structural Engineering. 15(4) 407-417.

[19] De Lorenzis, L., 2004, “Anchorage length of near-surface mounted fiber-reinforced polymer rods for concrete strengthening-analytical modeling”, ACI Struct. J. 101(3), 375–384.

[20] De Lorenzis, L. Teng J.G. 2007, “Near-surface mounted FRP reinforcement: An emerging technique for strengthening structures”, Composites Part B: Engineering. 38(2), 119-143.

[21] Seracino, R., Raizal Saifulnaz, M.R., and Oehlers, D.J., 2007 “Generic debonding resistance of EB and NSM plate-to-concrete joints”, J. Compos. Constr. 11(1), 62–70.

[22] Seracino, R., Jones, N.M., Ali, M.S.M., Page, M.W., and Oehlers, D.J., 2007, “Bond strength of near-surface mounted FRP strip-to-concrete joints”, J. Compos. Constr. 11(4), 401–409.

[23] CAN/CSA-S806-12 2012, “Design and construction of building components with fiber-reinforced polymer”, Canadian Standards Association, Rexdale, Canada.

[24] Khalifa, A., Gold, W.J., Nanni, A., and Aziz, A., 1998, “Contribution of externally bonded FRP to shear capacity of RC flexural members”, J. Compos. Constr. 2(4), 195–203.

[25] Mofidi, A. and Chaallal, O., 2011, “Shear Strengthening of RC Beams with Epoxy Bonded FRP—Influencing Factors and Conceptual Debonding Model”, American Society of Civil Engineers, J. Compos. Constr. 15(1), 62-74.

[26] Pellegrino, C., and Modena, C., 2002, “Fibre-reinforced polymer shear strengthening of RC beams with transverse-steel reinforcement”, J Compos Constr 6(2), 104–111.

[27] Pellegrino, C., and Vasic, M. (2013). Assessment of design procedures for the use of externally bonded FRP composites in shear strengthening of reinforced concrete beams. Compos. Part B: Eng. 45(1), 727-741.

Table Captions

Table 1 Accuracy of the predicted V_f of the existing models when compared to the existing experimental results.

Figure Captions

Figure 1 Number of tested specimens in the database versus failure modes with regards to cross-sectional shape of FRP NSM reinforcement
Figure 2 Average FRP shear contribution of specimens with regards to the internal steel stirrup reinforcement ratios
Figure 3 Shear contribution of NSM FRP (V_f) versus the applied shear
Figure 4 Shear contribution of transverse steel reinforcement (V_s) versus the applied shear
Figure 5 Calculated results using the proposed model versus experimental results considering all strengthened specimens with NSM FRP laminates and rods
Figure 6 Calculated results using the proposed model versus experimental results considering strengthened specimens with NSM FRP laminates only
Figure 7 Calculated results using the proposed model versus experimental results considering strengthened specimens with NSM FRP rods only

Table 1— Accuracy of the predicted V_f of the existing models when compared to the existing experimental results.

	R^2 (all specimens)	R^2 (NSM Laminates)	R^2 (NSM Rods)	V_{fcal} / V_{fexp}
Proposed model	0.64	0.67	0.65	0.80
De Lorenzis and Nanni (2001)	-	-[1]	0.34	0.90
Dias and Barros (2013)	-	0.44	-[2]	1.17
Anwarul Islam (2009)	< 0.10	< 0.10	< 0.10	1.91

1: De Lorenzis and Nanni (2001) model can only predict V_f for beam strengthened with NSM FRP rods.
2: Dias and Barros (2013) model can only predict V_f for beam strengthened with NSM FRP laminates.

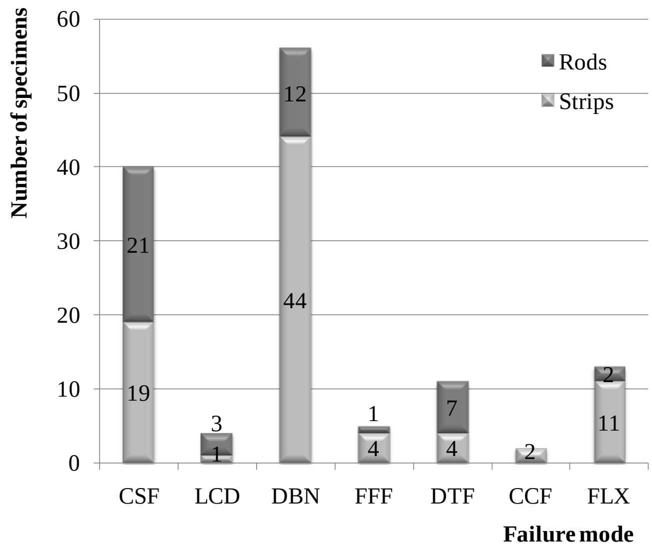

Figure 1 — Number of tested specimens in the database versus failure modes with regards to cross-sectional shape of FRP NSM reinforcement.

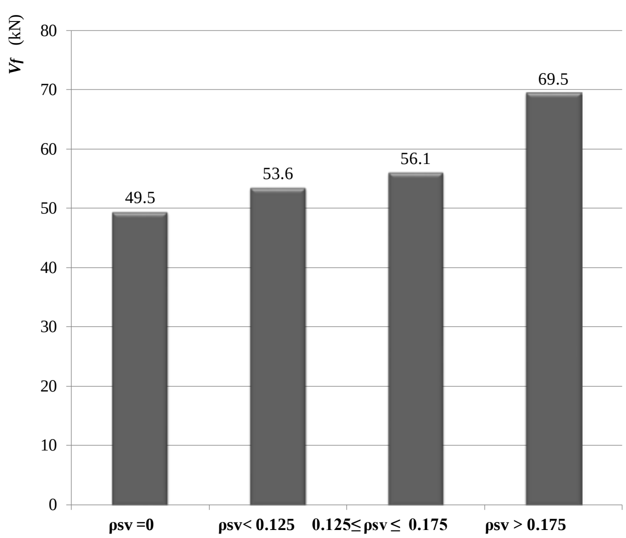

Figure 2 — Average FRP shear contribution of specimens with regards to the internal steel stirrup reinforcement ratios (1 kN is equal to 0.225 kip).

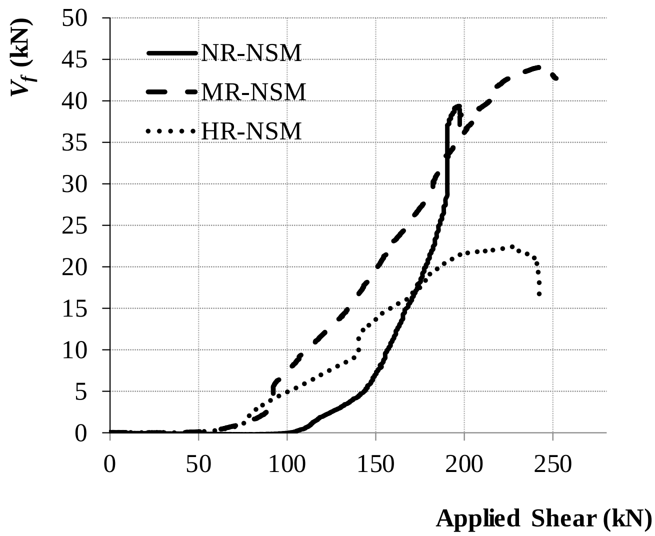

Figure 3 — Shear contribution of NSM FRP (V_f) versus the applied shear (1 kN is equal to 0.225 kip).

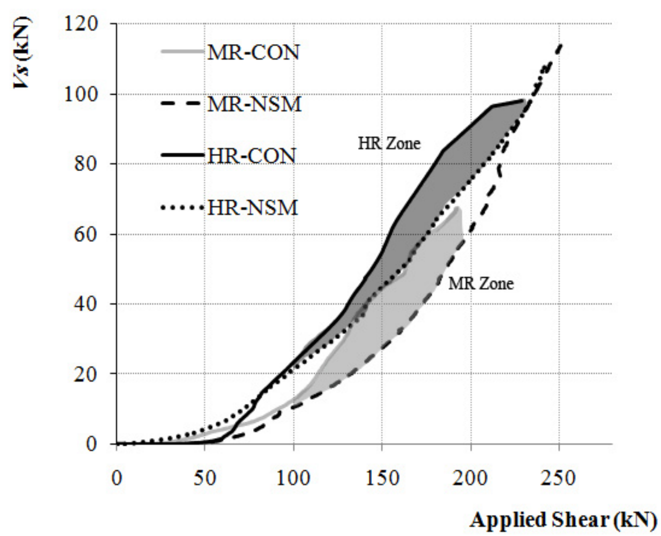

Figure 4 — Shear contribution of transverse steel reinforcement (V_s) versus the applied shear (1 kN is equal to 0.225 kip).

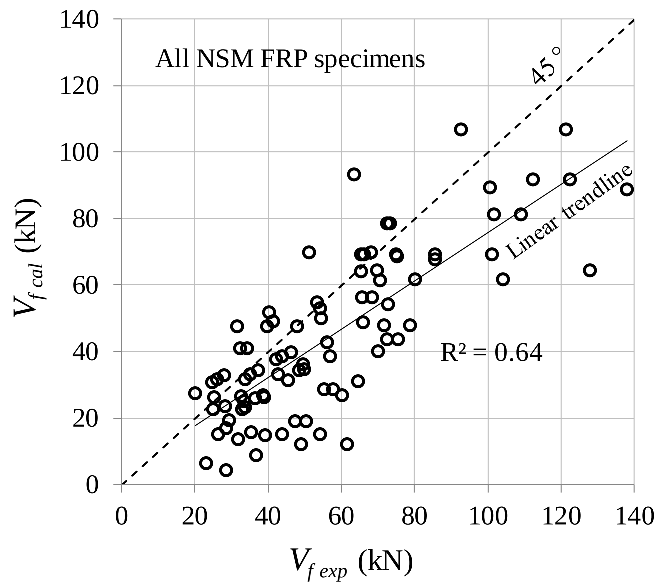

Figure 5 — Calculated results using the proposed model versus experimental results considering all strengthened specimens with NSM FRP laminates and rods (1 kN is equal to 0.225 kip).

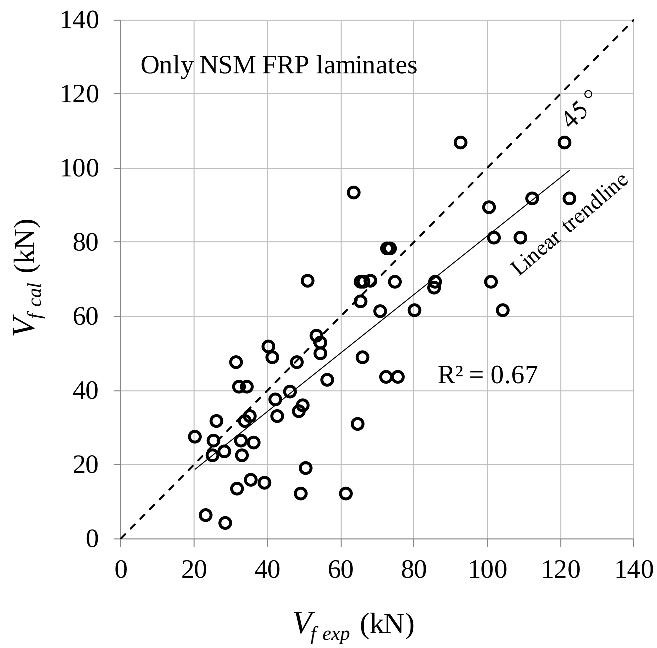

Figure 6 — Calculated results using the proposed model versus experimental results considering strengthened specimens with NSM FRP laminates only (1 kN is equal to 0.225 kip).

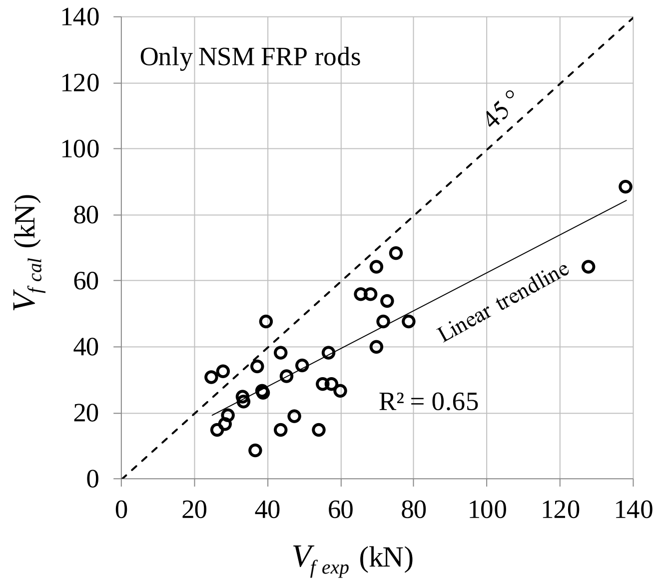

Figure 7 — Calculated results using the proposed model versus experimental results considering strengthened specimens with NSM FRP rods only (1 kN is equal to 0.225 kip).